REVIEW

Wearable patches for transdermal drug delivery

Jiahui He[a],[†], Yuyue Zhang[a],[†], Xinge Yu[a],[b], Chenjie Xu[a],[*]

[a]Department of Biomedical Engineering, City University of Hong Kong, Hong Kong 999077, China
[b]Hong Kong Centre for Cerebro-Cardiovascular Health Engineering, Hong Kong 999077, China

Abstract Transdermal drug delivery systems (TDDs) avoid gastrointestinal degradation and hepatic first-pass metabolism, providing good drug bioavailability and patient compliance. One emerging type of TDDs is the wearable patch worn on the skin surface to deliver medication through the skin. They can generally be grouped into passive and active types, depending on the properties of materials, design principles and integrated devices. This review describes the latest advancement in the development of wearable patches, focusing on the integration of stimulus-responsive materials and electronics. This development is deemed to provide a dosage, temporal, and spatial control of therapeutics delivery.

---

*Corresponding author.
E-mail address: chenjie.xu@cityu.edu.hk (Chenjie Xu).
[†]These authors made equal contributions to this work.

1. Introduction

Conventional drug delivery systems, including oral and parenteral delivery, suffer from hepatic first-pass metabolism, gastrointestinal degradation, and poor controllability of drug biodistribution. Transdermal drug delivery (TDD) allows the medicine to penetrate the stratum corneum (SC) and reach the epidermis and dermis layers for local and systemic therapy. The research can be dated back to the 1960s, when SC was found to be impeditive against water loss and skin penetration[1,2]. In 1975, researchers realized that the penetrability across the SC layer varied among different molecules, which could be modulated and controlled by optimizing the formulations[3]. In the following decades, hundreds of TDD formulations have been developed, providing higher drug bioavailability, better wearability and patient compliance (Fig. 1). These TDD platforms can be generally grouped into passive and active types[4,5]. Passive delivery refers to the spontaneous degradation of drug reservoir or diffusion-based drug release. Active delivery refers to the drug release induced by internal or external stimuli like the enzymes, pH, electrical[6], mechanical (ultrasound)[7], and optical fields[8]. Compared to passive delivery, active delivery releases drugs at target sites in a controlled spatial, temporal and dosage accuracy. The representative examples include the glucose-responsive insulin release microneedle (MN) patches[9], the smart-phone-controlled MN system for glucose management[10].

These active and passive TDDs can be grouped into patches, semi-solid formulations (cream, gel, ointments), and liquid formulations (spray, lotion). Liquid and semi-solid formulations are relatively easy to apply and can cover large area without being limited by skin area and curvature. However, they're relatively messy, their ingredients can be transferred easily to other areas of the skin that might not want to be touched, and they are challenging to apply in a precise dosage. On the another hand, patches can specifically act on the area in contact with the precise control of dosage applied. The first TDD patch (*i.e.*, Transderm Scop) was approved in 1979 by the U.S. Food and Drug Administration (FDA) for delivering scopolamine against motion sickness[11]. Since then, many TDD patches have been approved for vaccination, pain relief and skin management[12,13].

Recently, wearability has become a new trend in the development of TDD patch. The "wearability" addresses the factors that affect the degree of comfort the wearer or patient experiences while wearing the patch, including physical, psychological, and social aspects. It involves the use of new materials and designs that improve the wearability and comfort level. This review highlights the latest developments in the formats of adhesive hydrogel patches, MNs, and wearable electronics.

Besides the drug delivery function, they can also be used for sensing physiological information like body temperature[14], blood sugar level[15], lactic acid[16], pH, ions[17] and so on. We start with a brief description of the skin anatomical structure, and then discuss the different release mechanisms in TDD. Later the design concepts of different wearable patches for TDD are mentioned with a detailed iteration of current achievements and challenges.

2. Anatomical structure of the skin

The skin could be roughly split into the SC and epidermis, dermis, and hypodermis layers from surface to bottom (Fig. 2)[18]. The SC layer (10−20 μm) is a dense layer on the top of the epidermis, consisting of corneocytes and a lipid matrix. The corneocytes are tightly interconnected by corneodesmosomes, forming a mechanically stable barrier that protects the inner side from pathogen invasion, ultraviolet radiation, and loss of water. The epidermis (50−100 μm) is a non-vascularized matrix which mainly composed of keratinocytes, Merkel cells and Langerhans cells. Dermis (1−2 mm) contains a dense capillary network interconnecting with systemic circulation and is known as the first entrance for drug absorption. The hypodermis is the bottom layer of the skin, consisting of vascularized, loose, areolar connective tissue and adipose tissue.

A non-formulated and topically applied drug enters the skin mainly through the transepidermal and transappendageal pathways[19]. By the transepidermal way, drugs permeate either through intercellular lipid matrix (intercellular pathway) or through the corneocytes followed by intercellular lipid matrix (intracellular and transcellular pathway)[20]. However, studies show that the intercellular lipid matrix is the main obstacle to drug absorption, which especially makes it very challenging for those hydrophilic and large molecules to enter the skin[21]. The transappendageal pathways are to pass through the skin appendages, such as sebaceous glands and hair follicles. Compared to transepidermal pathways, it bypasses the lipid matrix. However, the surface area occupied by skin appendages is limited to around 0.1% of the total skin, and their numbers vary among different body parts and individuals, leaving challenges to predict or estimate the dosage entering the body.

To enhance drug penetration across the skin and the ultimate bioavailability, scientists and engineers develop many chemical, physical and biological methods. Chemical penetration enhancers include organic solvent, fatty acids, surfactants and nanoparticles[22]; physical enhancers include laser ablation, ultrasound, electrical field, heating, and MNs[23]; there are also biological
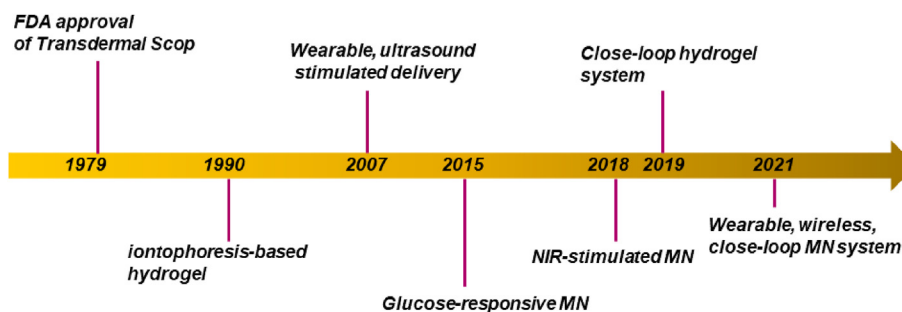

Figure 1 The timeline of transdermal drug delivery (TDD) systems development.
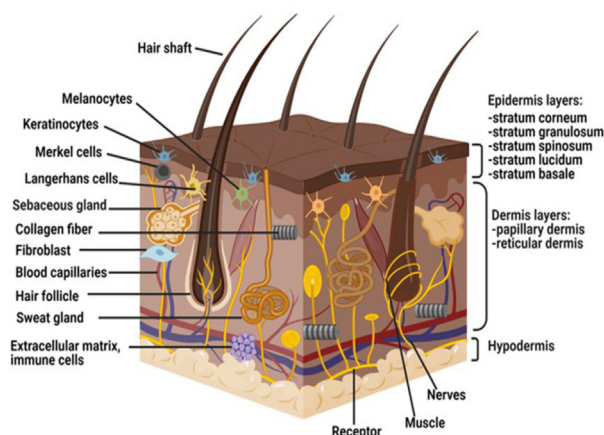
Figure 2 Schematic illustration of the skin anatomical structure (Reprinted with permission from Ref. 18. Copyright © 2021 MDPI).

molecules such as peptides to facilitate the skin penetration of drugs. The dosage of these enhancers should be carefully controlled to avoid potential skin irritation and damage.

3. Release principles of TDDs

3.1. Passive delivery

Passive delivery refers to the natural biodegradation/dissolution of drug reservoirs or passive diffusion of drugs from the reservoirs into the skin. The function and efficiency of passive delivery are determined by the formulation properties (hydrophobicity, charge, molecular weight, crystallinity and so on), dosage of active compounds, and skin conditions. For example, cationic chitosan formed a much stronger binding with protein agents than anionic sodium alginate[24−26], which provided a slower release profile. Hyaluronic acid (HA) is expected to degrade much faster *in vivo* than polyesters[27] or silk fibroin[28], which would provide a faster release of the encapsulated drugs. The degradation of TDDs can also be affected by the skin conditions like skin thickness, pH, temperature, and microbes on the surface. For example, the hydrocortisone-loaded microparticles (a pH-responsive polymer that dissolves at pH 6) didn't release drugs at normal (intact) skin pH (5.0−5.5). However, the delivery could be triggered on the atopic dermatitis skin where the pH was elevated[29].

However, regardless of the formulation, drug dosage and skin condition, one thing in common for all passive drug delivery is the reliance on Fick's law, which is to estimate the diffusion kinetics and optimize the molecule transportation[30]. As given by Eq. (1):

$$\frac{\mathrm{d}q}{\mathrm{d}t} = -DA\frac{\mathrm{d}c}{\mathrm{d}t} \tag{1}$$

where q is quantity of solute, A is membrane surface area, c is concentration; D is diffusion coefficient, $\frac{\mathrm{d}c}{\mathrm{d}t}$ is concentration gradient, the Fick's law presents the relationship between flux and impact factors. It points out that drug diffusion speed is determined by the concentration gradient, skin properties and thickness, and the interface area. Of course, other factors like skin surface temperature, pH and molecular weight of drugs also have specific influences. For example, Abdullah et al.[31] achieved a sustained and zero-order release of diclofenac sodium by controlling the drug gradients in their polyvinyl alcohol (PVA) patch. They selected Eudragit RS100 to prepare a rate-limiting membrane with

diclofenac sodium. The drug concentration in the matrix was constant, far higher than the saturation solubility; herein, the release rate was maintained for a long time. The patch realized a sustained release for 12 h *in vivo*, following zero-order kinetics with a value of 0.9753, and non-Fickian diffusion with a value of 0.949.

3.2. Active delivery

Active delivery refers to the delivery systems responsive to stimulants like electricity, ultrasound, light, etc. Electrically assisted delivery mainly makes use of iontophoresis and electroporation[32]. Iontophoresis uses a mild and continuous electrical current through the skin, allowing ionized or charged particles to cross the normal skin barrier. Uncharged and weakly charged molecules can also move with the bulk flow of the solvent generated by the preferential movement of mobile cations (electroosmosis). Different from iontophoresis, electroporation applies short (<ms), high-voltage pulses (≥100 V) to create transient pores on the skin[33]. The delivery efficiency in both cases can be controlled by pulse parameters (waveform, duration, amplitude), and drug properties [oil-water partition coefficient (log$P$), pKa and solubility][34,35].

Ultrasound has high directionality and penetrability through human tissue. The ultrasonic cavitation effect results in the formation, oscillation and collapse of microbubbles, leading to the disruption of lipid bilayers of SC[36]. The microbubble oscillation and associated acoustic streaming can significantly promote the passive diffusion of either dissolved molecules or nanoparticles in a low-viscosity solution.

The light-stimulated delivery is attractive due to accurate controllability. The applicable electromagnetic wave ranges from infrared light (NIR, 750−2000 nm), visible (400−750 nm) to ultraviolet (UV, 200−400 nm). However, UV light is less common in the transdermal field due to the poor tissue penetration depth and carcinogenic risk. Comparably, NIR is studied the most due to good penetration in deep tissue and fewer side-effect. To improve the spatiotemporal controllability, nanomaterials like gold nanoparticles, graphene, and quantum dots can be encapsulated to improve light absorption[5].

4. Wearable patch for passive delivery

4.1. Hydrogel patch

Hydrogel allows the ease-modification of the chemical, physical and biological properties. In transdermal delivery, the semi-solid morphology of hydrogel is also suitable for drug loading and release. At the same time, transdermal drug delivery is a non-invasive but effective drug delivery method as it is easy for self-administration and could bypass the first-pass hepatic metabolism. For example, Zhang et al.[37] reported a hybrid hydrogel platform that is capable for transdermal delivery of insulin and successfully realizes blood glucose level management in diabetic mice models. The carrier of the hybrid hydrogel is arginine-based poly (ester amide) (Arg-PEA), which is positively charged that can absorb protein drugs, has good biocompatibility and can form hydrogel scaffold with polyethylene glycol diacrylamide (PEG-DA) by UV photocrosslinking. It has been proved in previous research that transdermal peptides, such as sTD1, can significantly improve the transdermal drug delivery of therapeutic macromolecules[38]. The insulin and TD1 were pre-loaded into the solution before crosslinking and thus could realize a sustained release after application. *In vivo* experiments on STZ-induced diabetic mice models have

proved that in comparison with blank hydrogel, the insulin-loaded hybrid hydrogel can significantly reduce the blood glucose level from 23.63 to 12.63 mmol/mL after 4 h, indicating the successful release and transdermal delivery of insulin.

Here we classify the hydrogel patches into adhesive hydrogel patch and stimulus-responsive hydrogel patch.

4.1.1. Adhesive hydrogel patch

A tight binding between the hydrogel patch and skin, could prevent potential intrusion of contaminants like bacteria and enable a stable drug release into the skin. Pressure-sensitive adhesive (PSA) hydrogel can adhere to the skin under pressing and leave no residue after peeling off. Typical PSA hydrogels include poly-ethylene glycol (PEG), high molecular weight polyvinyl pyrrolidone (PVP), polyacrylamide, polydopamine and their derivatives[39,40]. For example, Jung et al.[41] developed a PSA hydrogel using polyacrylamide/polydopamine (PAM/PDA) and mesoporous silica nanoparticles (XL-MSNs) (Fig. 3a). The adhesive energy of the PAM/PDA/XL-MSN reached 15.3 J/m^2, around 3 folders higher than PAM/PDA gel. This is due to the presence of XL-MSNs. Later, the model drug R6G was continuously released from the patch to porcine skin for a period of 24 h. The penetration depth was up to 2250 μm, which benefited from the tightly binding interface between gel and skin. Liu et al.[42] reported a novel hydrogel dressing that is both anti-infectious and can improve new vasculature at the wounded area as well. The hydrogel dressing has a core-shell structure that is combined by electrostatic interactions. The outer layer is alginate (SA) hydrogel loaded with silver nanoparticles (AgNPs) which can prevent infection, while the inner layer is chitosan (CS) hydrogel loaded with sodium alginate micro-spheres (ArgMS) which contains L-arginine that could be sustained released to promote vascular regeneration. It has been proved that compared with blank hydrogel, the SA-AgNP/CS-ArgMS hydrogel is beneficial with diabetic wound healing as it could vastly improve the re-epithelialization, collagen deposition, granulation tissue formation as well as angiogenesis.

4.1.2. Stimulus-responsive hydrogel patch

Stimulus-responsive hydrogel patch changes its chemical or physical properties upon the stimulation of pH, temperature, light, etc. The property change would influence the drug release
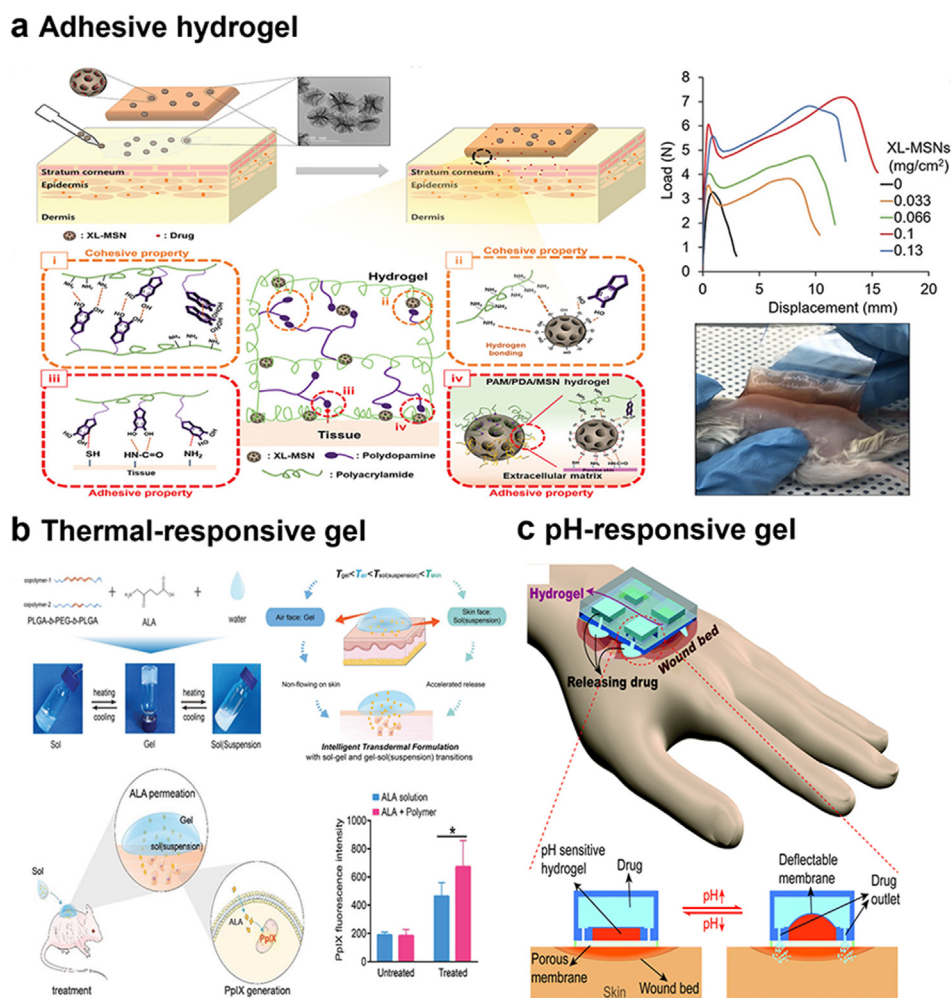
Figure 3 Hydrogel patch in TDD. (a) Polyacrylamide/polydopamine (PAM/PDA) hydrogel with epidermal adhesion (Reprinted with permission from Ref. 41. Copyright © 2020 Wiley). (b) The thermogel for transdermal delivery of 5-aminolevulinic acid (ALA) (Reprinted with permission from Ref. 43. Copyright © 2021 Wiley). (c) A pH-responsive hydrogel patch for treating chronic wounds (Reprinted with permission from Ref. 45. Copyright © 2019 Royal Society of Chemistry).

profile from the patch. For example, Cao et al.[43] reported a PLGA/PEG thermogel for delivering 5-aminolevulinic acid (ALA) (Fig. 3b). This material gelled at sol-gel transition temperature (T_{gel}) and became solutions at the gel−sol transition temperature ($T_{sol\ (suspension)}$). (T_{gel} < room temperature < $T_{sol\ (suspension)}$< body temperature) At the air-patch interface, it was the gel with limited water evaporation and morphology change. At the skin-patch interface, it was liquid, rendering the diffusion of ALA from patch to the skin. Martí-Centelles et al.[44] reported an acid-responsive hydrogel patch to treat inflamed skin tissues. The hydrogel was made of charge complementary amphipathic tetra-peptides of alternating hydrophobic and hydrophilic amino acids. The anti-inflammatory drug, (S)-naproxen (Npx), was integrated into the gel components by $\pi-\pi$ bond and hydrophobic effect, its electrostatic interactions with gel were pH-responsive, which would become weaker under pH 5 than that of pH 7, resulting in rapid release. Jiang et al.[45] designed a flexible and wearable patch composed of the PDMS as the drug reservoir and the pH-responsive gel poly (methacrylic acid-co-acrylamide) [poly (mAA-co-AAm)] as the contacting layer with skin (Fig. 3c). When the gel was exposed to the alkaline pH of an infected wound, the carboxyl group (−COOH) of MAA was ionized to −COO⁻, increasing the internal electrostatic repulsion of the polymer network and leading to the gel swelling and faster drug release. The device was able to release an aqueous, anti-bacterial solution (<0.1 μL/min) upon the change of pH from 5 to 7[46]. Bao et al.[47] reported a hybrid hydrogel that is sensitive to acid and can provide controllable stiffness and calcium supply, which can significantly promote bone regeneration. The proposed hydrogel was Pluronic F127 (purchased from Sigma) that diacrylated by condensation, which is capable of easy formulation and has great biocompatibility. Nano-$CaCO_3$ was introduced into the hydrogel in a space-controllable distribution as it could not only provide sufficient mechanical properties of the hydrogel but also provide calcium ion supply in a weak acid environment that is beneficial to bone regeneration. The nano-$CaCO_3$ is located in the core area of the F−Ca-A hydrogel. Under a weak acid environment, the gradient distribution of calcium ions in the hybrid hydrogel could be slowly released and thus promote the differentiation of osteo-blast and the regeneration of new bone. In a New Zealand rabbit skull defect model, the newly generated bone of the F−Ca-A hydrogel-treated group shows higher continuity and thickness compared with the blank F-A hydrogel within 8−12 weeks. This acid-sensitive hydrogel would have a broad application future in the design and fabrication of hydrogel scaffolds for bone regen-eration. Despite pH-sensitive hydrogel, the hydrogel dressing combined with photo therapies also has great application potation in wound healing. The hydrogel dressing offers a moist environ-ment that is beneficial for wound healing, while at the same time, the phototherapy could improve the release of containing drug and thus provide an anti-infectious, high-efficient and low-irritant method to improve wound healing[48]. Li et al.[49] reported a hydrogel showing superior anti-bacterial efficacy for skin regen-eration under the irradiation of NIR light. The hydrogel was composed of 3-(trimethoxysilyl)propyl methacrylate (MPS, 97%) and mesoporous silica ($mSiO_2$) modified CuS nanoparticles. Under 808 nm NIR light irradiation, the hydrogel could realize a controlled release of the Cu ions, improving angiogenesis and providing the anti-bacterial property against *Staphylococcus aureus* and *Escherichia coli*.

4.2. Microneedle patch

MNs are miniature minimized needles with dimensions of tens to hundreds of micrometers that can mechanically break superficial skin layers to improve drug permeation[50]. Relative to the skin area, MNs are usually small and have limited drug-loading ability. "Poke and patch" is one way to solve the dosage issue. Yang et al.[51] reported a touch-MN array patch (TMAP) for insulin de-livery using the "poke and patch" strategy (Fig. 4a). TMAP mainly consisted of PMMA MNs and an insulin-loaded sponge. Touching the tape pushed MNs to penetrate through the sponge and skin. Only when holding the pressing, the insulin in the sponge would diffuse through the micro-holes into the skin. The release rate was controllable *via* touching pressure and frequency. Animal studies showed that two steps of touching-induced release *via* TMAP achieved corresponding normoglycemic times up to 12 h, which was around 2.5-fold of that of insulin injection. TMAP treatment also reduced the risk of hypoglycemia. However, there is one issue related to this "Poke and patch" method for insulin delivery. The management of diabetes requires the accu-rate control of blood glucose. In other words, the insulin dosage delivered should match the actual blood glucose level (BGL) of the patient, which is hard to realize through the dosage-fixed MN patch.

Another strategy, "coated and poke" is to deliver drugs by pre-coating them on the MN tips, which is suitable for rapid release and small dosage. Choi et al.[52] developed HA MNs coated with the Canine influenza vaccine (Fig. 4b), which could partially maintain bioavailability even at 50 °C for 3 weeks. In the guinea pigs, MNs elicited antibody responses and reduced viral shedding. The hemagglutination inhibition antibody was 2-fold higher than that of intramuscular injection. Similarly, nucleic acids can be delivered by MNs as well. Wang et al.[53] developed a mesoporous silica ($mSiO_2$) coated HA MNs. The siRNA-loaded $mSiO_2$ shell can effectively protect the siRNA from enzymatic degradation, and the endosome−lysosome degradation axis. Luminescence imaging presented that the $mSiO_2$ nanoparticle (around 50 nm) successfully across the micro holes created by HA MNs and released the cargo in the skin model. The MNs were used to deliver siRNA targeting transforming growth factor-beta type I receptor (TGF-βRI), which led to the silencing of TGF-βRI expression in hypertrophic scar-derived fibroblasts.

"Poke and flow" approach refers to delivering the drugs through the inner cavity of hollow MNs. The hollow structure is normally carved by highly definitive processing like reactive ion etching and laser etching. Bolton et al.[54] fabricated a hollow sil-icon MN array using dry plasma processing. The sub-millimeter construction and the sharp beveled tip minimized the insertion force, reducing the pain of injury. Resnik[55] designed a hollow MN patch driven by a micro pump, and demonstrated that the release rate of model drug and insulin was found to predominantly depend on the flow rate of drug fluid. The drug transport efficiency of this device was limited by the inability of the viable epidermis to absorb and the low density of capillary under skin. Yeung[56] designed a hollow MN patch coupling with a microfluid chip for the delivery of multiple drugs (Fig. 4c). The patch was fabricated by UV-curing resin using Stereolithography (SLA) 3D printing. The dosage of model drugs delivered into the skin was tunable by adjusting the flow rate with an electrical controller[57]. With the derived template, they were able to make hollow MNs of
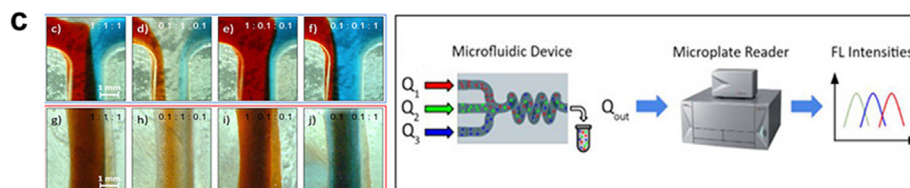
Poke and patch

a

Coated and poke

b

Poke and flow

c
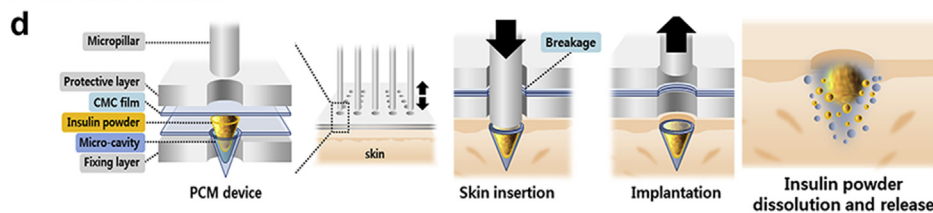

Poke and release

d
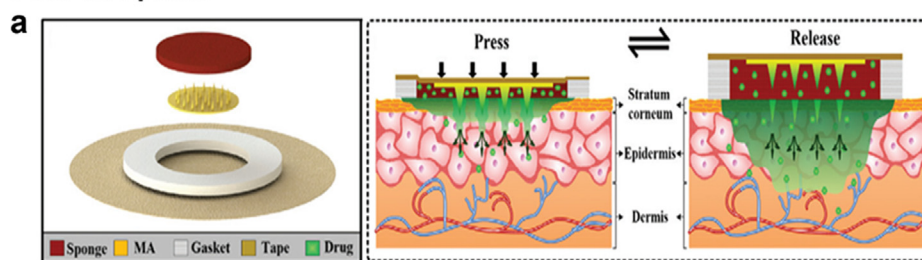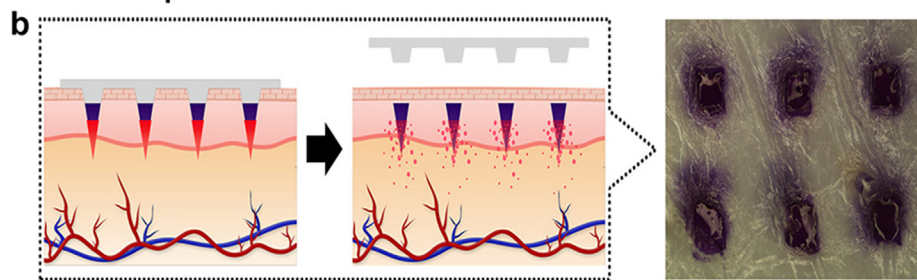
Figure 4 MN patch for TDD. (a) The touching-induced MN patch integrating with external insulin-loaded nanovesicle (Reprinted with permission from Ref. 51. Copyright © 2018 Taylor & Francis group). (b) HA MNs coated with Canine influenza vaccine for rapid immune response (Reprinted with permission from Ref. 52. Copyright © 2018 Elsevier). (c) A microfluid chip coupled with the hollow MN patch for the delivery of multiple drugs (Reprinted with permission from Ref. 56. Copyright © 2019 MENU). (d) Dissolving MN patch for high-dosage insulin delivery (Reprinted with permission from Ref. 60. Copyright © 2020 Elsevier).

polymethyl methacrylate (PMMA), polystyrene, and epoxy resin. These MNs exhibited a nearly consistent puncture force of around 1.03 N per needle tip for penetrating rabbit skin. MNs loaded with prostate cancer vaccine could successfully trigger the immune response of mice (>60% antibody of hypodermic injection with an end-point titer at the ratio of 1:1000). Besides 3D-printing, laser cutting, reactive ion etching (RIE) are also suitable for hollow MNs fabrication[58]. However, laser cutting and RIE are limited by the high cost.

"Poke and release" type MNs provide an enclosed environment for contained drugs. The drug release rate depends on the drugs' diffusion and degradation/swelling of MN material. MNs made of PVP, PVA, carboxymethyl cellulose (CMC) and HA dissolve within seconds to minutes, while those made of chitosan, PLGA, and PCL need several weeks to months[59]. Kim[60]

fabricated CMC MNs to deliver high-dosage insulin (Fig. 4d). The insulin-loaded tips can be rapidly immersed into the skin by a specialized tool, then the insulin was fully released within 4 h. Briefly, the CMC solution was first deposited onto the MN mold by centrifugation, and dried to formed a thin, rigid shell, followed by loading the high-dosage insulin powder into the micro-cavities, upon the CMC shell. Finally, the insulin-filled cavities were encapsulated by a layer of CMC film. Due to the separation of MN fabrication and dry-loading method, the insulin can maintain great bioactivity during processing and longer storage. Li et al.[61] designed a rapid-separated MN using PLGA/PLA composite for the sustained release of a contraceptive. The release of contraceptives was adjustable by modifying the ratio of PLGA/PLA, which can be up to 40 days for levonorgestrel (LNG) delivery. The latest innovation is a glucose-responsive closed-loop delivery

system of insulin and glucagon for stable self-management of blood sugar level over 22 h[62]. On a hyperglycemic model (mice), the increasing binding between glucose-responsive phenylboronic acid units and glucose inside the crosslinked HA MNs, reversibly shifted the net charge of the MN matrix. As a result, there was a faster and slower release ratio of the negatively charged insulin and the positively charged glucagon analog from the MNs, turning the condition back to euglycemia. Some of these bio-responsive MNs for insulin delivery have been seen in clinical trials[9,62,63].

5. Wearable patch for active delivery

5.1. Electricity-stimulated patch

Wearable patch integrating electronics allows the precise control of drug delivery through electric signaling. The microprogrammed control unit (MCU) brings accurate management of drug application. For example, Xu et al.[64] designed a software-controlled wearable device to assess/treat wound infections and facilitate wound healing (Fig. 5a). Near Field Communication (NFC) antenna was integrated into the flexible printed circuit to control the drug-containing adhesive patch and biosensing modules. Mediated by a near-field coil, the device was remotely controlled and powered. The sensing module could monitor the temperature, pH, and uric acids on the infection sites. Hydrogel is also suitable for constructing electricity-stimulated wearable devices. Lim et al.[65] developed a hydrogel patch composed of impedance sensors, an electrical nerve stimulator, a transcutaneous oxygen pressure sensor and iontophoretic electrodes (Fig. 5b). The tissue-like, conductive PEDOT: PSS/PAAM hydrogel patch not only served as a skin-interfaced substrate but also provided stable electrolytes for electrochemical sensing and iontophoresis-based drug delivery. Compared with conductive PAAM gel, the impedance was reduced by around 20% under a low-frequency electrical field. AgCl cathode and Zn anode were integrated into the hydrogel for powering iontophoresis, which constantly generated 200 μA current for more than 100 min. In vitro test showed around 500 folds of current density (1 Hz) via the self-powered iontophoretic patch compared to the control PAAM gel. This permitted a deeper penetration (630 μm) in porcine skin for the model drug (Rhodamine B) via the self-powered iontophoretic patch that used natural diffusion (350 μm).

MN is also widely used in wearable device to improve the skin penetration of drugs. Li et al.[66] reported an electroporation method built on MNs for transdermal gene delivery (DNA plasmid of red fluorescent protein, RFP). They fabricated a conductive MN array as the electrode to apply the tri-phase electric pulsing. Before the electroporation, hyaluronidase and RFP plasmid were injected into the unhaired thing of the mouse stepwise. They examined the influence of voltage (30−90 V) and length of MN tips (0.6 or 1.2 mm). There was an optimal voltage (50 V in their case), which could provide a higher transfection rate and minimal cell damage. The shorter device also provided better results in transfection. Kusama et al.[67] reported a conductive and porous MN patch integrated with flexible carbon fabric and fructose/O_2 battery. The porous cavity was filled with conductive polymer, poly-2-acrylamido-2-methylpropane sulfonate (PAMPS), which reduced the resistance of skin (100 kΩ). With the current (up to 0.2 mA/cm^2) generated by an enzyme battery, the PAMPS and

epidermal tissue built up a negatively charged channel to generate electroosmotic flow that promoted the drug flow from MNs into the skin. Compared to the naked MN patch, the PAMPS-modified porous MN patch exhibited around 500 times transportation rate of FITC-dextran (10,000 Da).

The rigid, bulky powering component, as well as limited capacity, might hinder the overall performance of wearable electronics. Besides the wireless charging technology, self-powering is an alternative strategy[68]. For example, a triboelectric nano-generator (TENG) can power wearable devices by converting biomechanical energy from body motions into electrical energy. Wang's group[69] used TENG to provide electric pulses for electroporation. A hand-cranking revolution of this device in 1s generated an alternating current with open-circuit voltage, short-circuit current, and transferred charge of 20 V, 4 μA, and 0.06 μC, respectively. The silicon MNs were cleverly adopted as the output side to locally induce an enhanced electric field: around 2800 V/cm on each needle. As a proof of concept, the device was used to stimulate the electroporation on the breast cancer cells for the delivery of small molecules, macromolecules, and siRNA. In another case, researchers designed a flexible, piezoelectric film (PVDF)-integrated MN patch for psoriasis treatment (Fig. 5c)[70]. The MN was coated by a layer of Polypyrrole (PPy) [electrostatically bonding with the Dexamethasone (Dex)]. Rather than receiving energy from external devices and motions, general pressing or twisting the patch only would induce an electric pulse generated by PVDF, which stimulated the reversible redox of PPy film for the release of Dex. In view of the advantages of self-powered technology, motion-induced electric power for active delivery can potentially promote the miniaturization of wearable devices.

5.2. Ultrasound-stimulated patch

The ultrasound-responsive patch contains components that respond to either low frequency (<100 kHz) or high-frequency ultrasound (>100 kHz and MHz range). Since the 1990s, ultrasound has been shown to enhance the permeability of agents into cells and tissues mainly through thermal and non-thermal effect. The thermal effects are from the absorption of acoustic energy in tissues, while non-thermal effects are generated from ultrasound pressure, acoustic streaming, microjet, and cavitation etc.[36,71] In the wearable patch, the ultrasonic field can be induced by removal devices or integrated components, mediating the release of drugs from the reservoirs. Soto et al.[72] developed a wearable gel patch for lidocaine delivery based on acoustic droplet vaporization (ADV) (Fig. 6a). The lidocaine was mixed in perfluorocarbon emulsion and stored in a soft array of micro holes. The emulsion was vaporized by ultrasound pulse (25 ms, 2.25 MHz, and 12 V), producing high pressure to breach the dermal barriers and leaving micropores on the skin for lidocaine absorption. The delivered dosage of lidocaine was 4- and 2-hold higher than that of passive diffusion and ultrasound alone, respectively. To evaluate the potential of the device for chronic pain therapeutic, it is necessary to process a large-scale clinical validation targeting the different areas of the human body with varying nerve depths. Next, researchers expected to miniaturize the portable ultrasound probes, to improve the potential of this technology as a point-of-care medical device in clinical use. Choi et al.[73] found a reversible metal−tannic acid (TA) coordination that is responsive to
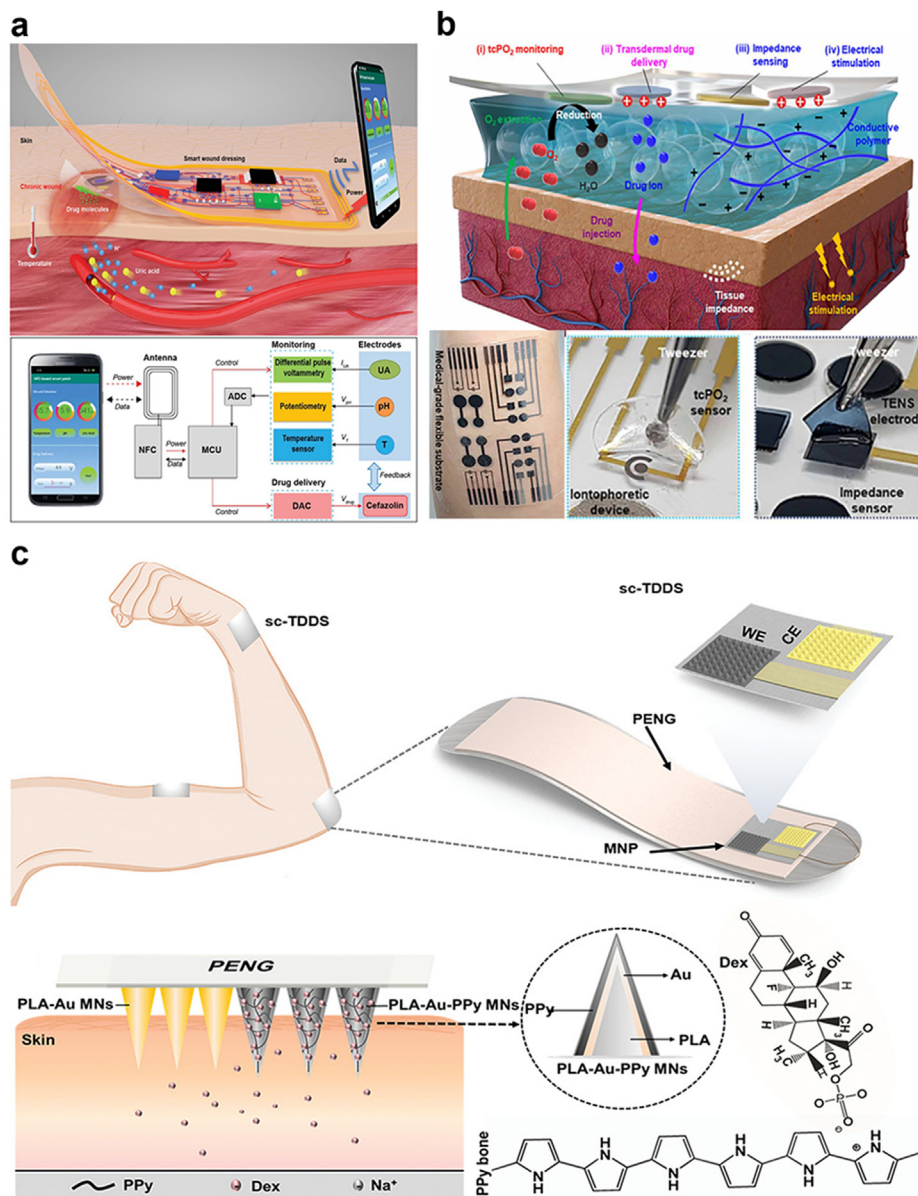
Figure 5 Electricity-stimulated wearable patch for TDD. (a) Battery-free and wireless wearable devices for wound infection monitoring and management (Reprinted with permission from Ref. 64. Copyright © 2021 Wiley). (b) Tissue-like, conductive hydrogel system for wearable biosensing and ionophoresis-based delivery (Reprinted with permission from Ref. 65. Copyright © 2021 AAAS). (c) Piezoelectric-based MN tape for delivering the anti-inflammatory drug (Reprinted with permission from Ref. 70. Copyright © 2021 Wiley).

ultrasound stimuli. They then coated the porous SiO_2 nanoparticles with Fe−TA network (TA−Fe^{III}/MSN), which were loaded into sodium alginate hydrogel (Fig. 6b). A skin patch was then made using this gel formulation. When low-frequency ultrasound was applied (50 Hz for 2 min), the Fe-TA bonding was destabilized, leading to network losing and drug release on skin.

Besides working alone, ultrasound can also cooperate with other devices like MNs. MNs first open up the skin barriers to macromolecules, and ultrasound enhances the diffusion of drug molecules. For example, Chen et al.[74] combined the Lead Zirconate Titanate (PZT) thin film, drug reservoir (for drug solution storing) and silicon hollow MNs into an ultrasound-responsive patch. The PZT film was used to generate the ultrasound

(20 kHz frequency, 0.5 W/cm^2), enabling the 9-fold faster release of model drugs (calcein and BSA) from the hollow MNs than the passive diffusion. Under ultrasonic powers from 0.1 to 6 W/cm^2, the temperature of the drug solution only increased about 1−3 C, leaving no damaging effect on the drug. Ning et al.[75] developed a type of MNs that created microbubbles through the reaction of citric acid and sodium bicarbonate (Fig. 6c). The bubble layer was fabricated *via* the frozen immersion method, which allowed the loading of both hydrophobic and hydrophilic drugs. Ultrasound was applied to enhance the generation of the bubbles further, leading to vortex flow to drive the drug passage. Despite the high efficacy of ultrasound, the excessive heating from a wearable device may lead to the variation in drug release rate and
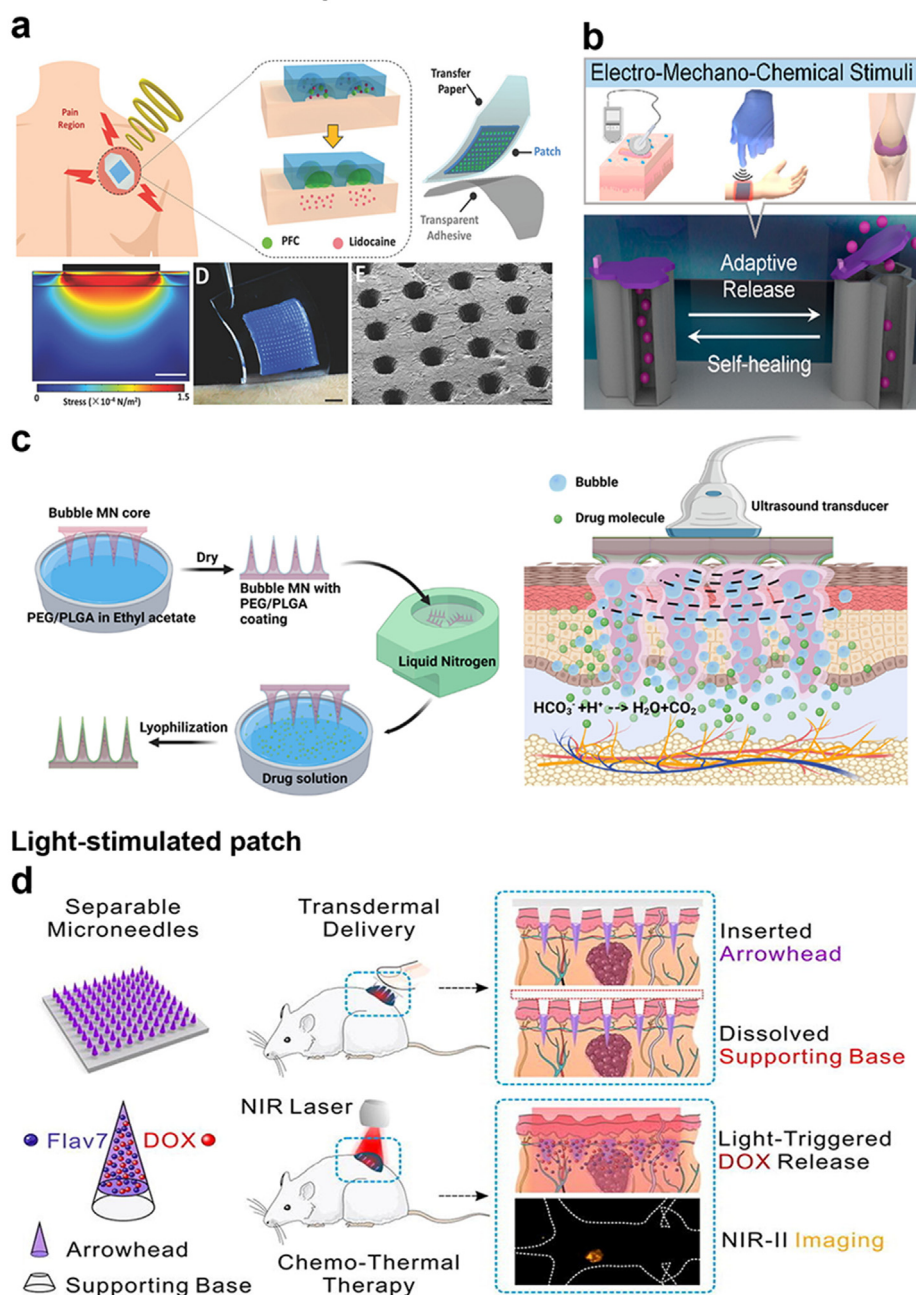
Figure 6 Ultrasound-based wearable devices for TDD: (a) Noninvasive delivery of lidocaine by acoustic droplet-vaporization-based wearable devices (Reprinted with permission from Ref. 72. Copyright © 2018 Wiley). (b) Electro-mechanochemical gating for controlled guest-release patches and injectable gels (Reprinted with permission from Ref. 73. Copyright © 2021 ACS). (c) Bubble-generating MN delivering photodynamic agent for transdermal cancer therapy (Reprinted with permission from Ref. 75. Copyright © 2021 ACS). (d) Flav7 + DOX co-loaded MN for light-triggered tumors treatment (Reprinted with permission from Ref. 79. Copyright © 2022 Elsevier).

skin irritation, which have been regarded by the FDA as a main issue[76]. Therefore, the programmable ultrasound is expected to control insertion depth and area accurately. An exciting example is from Chen et al.[77], who reported the programmable ultrasound-induced delivery. Their ultrasonic device produced highly-focused ultrasound to perforate the murine skin. They showed that the area and depth of skin penetration region could be mediated through ultrasound cycles, frequency and peak negative pressure. The highly focused ultrasound not only enabled adjustable penetration area from 0.078 ± 0.045 to 1.295 ± 0.279 mm^2 (Fig. 6d)[78] but also monitored the skin penetration by ultrasonic imaging. Therefore, the system can accurately control the release rate meanwhile avoid over-damage of the skin. In the application of vaccine delivery, the device had various penetration patterns with aligned micro holes. By adjusting the pattern, the vaccine doses could be adjusted.

5.3. *Light-stimulated patch*

The light-responsive system benefits from the accurate control of the light intensity and covering the area, leading to precise dosing. NIR light is the most popular light source because of the deep penetration in skin tissue and less damage to the tissue. Dhal et al.[46] adopted light-emitting $NaYF_4$ upconversion particles as a NIR-triggered ROS generator for skin cancer treatment. First of all, they made oleogels as the drug reservoir (using soybean oil as solution and stearic acid as gelation agents as well as permeation enhancers). Normal upconversion nanoparticle-based ROS therapy in the systemic circulation lack localizing ability. Thus it is still challenging to target those topical, deeply-seated lesions such as melanoma tumors. However, the oleogel can deeply deliver the nanoparticle into skin lesions, conducting the ROS generation in the deep side, and thus a significant bioavailability. The *in vitro* study presented that the subcutaneous and intradermal dosage of the nanoparticles delivered by the oleogels group was up to 9 $\mu g/cm^3$ within 48 h, while the non-gel group (directly smearing nanoparticle) had almost no subcutaneous or intradermal dosage. The 1,3-Diphenylisobenzofuran (DPBF) fluorescent probe assay (to measure ROS on light exposure.) detected higher ROS generated by the oleogels group (around 55% consumed DPBF), while the non-gel group presented little ROS production (around 0% consumed DPBF). Similarly, Wang et al.[79] developed a phase-change polycaprolactone (PCL) MN patch loaded with NIR-II fluorophore Flav7 and the antitumor drug doxorubicin (DOX) for tumor chemo-thermal therapy (Fig. 6d). The Flav7 has remarkable photothermal efficiency and fluorescence imaging ability. Under laser irradiation, Flav7 converted the light energy to heat and the PCL matrix melted, causing the release of DOX. In the animal study, the release of DOX from the MN patch led to intensive necrosis and apoptosis of tumors. As a conceptual study, researchers claimed that intensive optimization of the structure parameters was essential in future work, such as the length of drug-loaded needle tips.

6. Challenges and future development in the clinical translation

As often mentioned in the literature, the academic and medical fields believe that wearable devices would significantly improve patient compliance and life quality through achieving the dosage, temporal, and spatial control of therapeutics delivery. Successful cases include Duragesic® for fentanyl delivery, with global sales coming to $2 billion from 1990 to 2004, and Androgel® for testosterone replacement delivery, which generated $900 million in the USA in 2010[80]. However, challenges exist in the wide application of wearable devices to replace the existing formulations and devices.[12]

6.1. *Safety*

Wearable patches composed of multiple components require long-term interaction between skin tissue and the device. Issues often seen in the literature include the unstable physical/chemical properties of the patch or the residual left on the skin that may lead to skin irritation or damage. For example, FDA had raised the concern about the external physical field, such as heating, that may lead to the variation of drug release rate[76]. One way to minimize this issue is to use materials or components that have been components in the already approved medical devices or formulations.

6.2. *Complexity in the development*

Wearable TDD devices require the establishment of the new production line. While there is an existing production line of Microelectromechanical systems (MEMS) technology, the consistent integration of biomaterials, MCU, microstructured components and battery is challenging and requires collaboration between the chemical industry, pharmacological industry, microfabrication, and even IT.

6.3. *Consistency in application*

The drug delivery efficacy of the TDD system largely relies on the condition of the patients' skin, which is easily affected by age, location, and pre-treatment method, etc. Under the premise of ensuring safety, how to achieve a consistent delivery across a wide range of populations remains to be improved.

7. Outlook

This review summarizes the latest achievement in wearable patches to achieve a convenient, patient-friendly, and effective TDD. We group these devices into passive and active systems, depending on the properties of materials, design principles and integrated devices. For passive systems, we discussed hydrogel patches and MN patches. The active systems include those responsive to light, electric field, ultrasound and etc. These wearable TDD devices have found their applications in diabetes, skin diseases, birth control, wound healing, etc. While we are excited by these advances, there are still a lot of gaps for improvement that could be covered for TDD technology. For instance, evaluations of the side effect, efficacy as well as safety are needed to optimize the delivery system. We envision that the ongoing development of microfabrication, material science and medicine would be constantly induced to these fields, promising a brilliant hope to fight the global health crisis.

Author contributions

Chenjie Xu proposed the concept. Jiahui He, Yuyue Zhang, and Chenjie Xu wrote the manuscript. Xinge Yu gave comments on the manuscript. All authors have read and approved the final manuscript.

Conflicts of interest

The authors declare no conflicts of interest.

References

1. Scheuplein RJ. Mechanism of percutaneous adsorption: I. routes of penetration and the influence of solubility. *J Invest Dermatol* 1965;**45**: 334—46.

2. Blank IH. Penetration of low-molecular-weight alcohols into skin: I. effect of concentration of alcohol and type of vehicle. *J Invest Dermatol* 1964;**43**:415—20.

3. Michaels AS, Chandrasekaran SK, Shaw JE. Drug permeation through human skin: theory and *in vitro* experimental measurement. *AIChE J* 1975;**21**:985—96.

4. Bagherifard S, Tamayol A, Mostafalu P, Akbari M, Comotto M, Annabi N, et al. Dermal patch with integrated flexible heater for on demand drug delivery. *Adv Healthc Mater* 2016;**5**:175—84.

5. Amjadi M, Sheykhansari S, Nelson BJ, Sitti M. Recent advances in wearable transdermal delivery systems. *Adv Mater* 2018;**30**:1704530.

6. Padmanabhan RV, Phipps JB, Lattin GA, Sawchuk RJ. *In vitro* and *in vivo* evaluation of transdermal iontophoretic delivery of hydromorphone. *J Control Release* 1990;**11**:123—35.

7. Hsieh CH, Ku YA, Chiu LH, Young TH, Huang YY. A transdermal drug delivery system containing deferoxamine mesylate for the treatment of β-thalassaemia major. *Biomed Eng* 2011;**23**:29—35.

8. Zhang Y, Wang D, Gao M, Xu B, Zhu J, Yu W, et al. Separable microneedles for near-infrared light-triggered transdermal delivery of metformin in diabetic rats. *ACS Biomater Sci Eng* 2018;**4**:2879—88.

9. Yu J, Wang J, Zhang Y, Chen G, Mao W, Ye Y, et al. Glucose-responsive insulin patch for the regulation of blood glucose in mice and minipigs. *Nat Biomed Eng* 2020;**4**:499—506.

10. Li X, Huang X, Mo J, Wang H, Huang Q, Yang C, et al. A fully integrated closed-loop system based on mesoporous microneedles-iontophoresis for diabetes treatment. *Adv Sci* 2021;**8**:2100827.

11. Mali AD, Bathe R, Patil M. An updated review on transdermal drug delivery systems. *Int J Eng Sci* 2015;**1**:244—54.

12. Bird D, Ravindra NM. Transdermal drug delivery and patches—an overview. *Med Devices Sens* 2020;**3**:e10069.

13. Chen Y, Alba M, Tieu T, Tong Z, Minhas RS, Rudd D, et al. Engineering micro—nanomaterials for biomedical translation. *Adv Nanobiomed Res* 2021;**1**:2100002.

14. Yan C, Wang J, Lee PS. Stretchable graphene thermistor with tunable thermal index. *ACS Nano* 2015;**9**:2130—7.

15. Lee H, Song C, Hong YS, Kim M, Cho HR, Kang T, et al. Wearable/disposable sweat-based glucose monitoring device with multistage transdermal drug delivery module. *Sci Adv* 2017;**3**:e1601314.

16. Payne ME, Zamarayeva A, Pister VI, Yamamoto NAD, Arias AC. Printed, flexible lactate sensors: design considerations before performing on-body measurements. *Sci Rep* 2019;**9**:13720.

17. Cui X, Bao Y, Han T, Liu Z, Ma Y, Sun Z. A wearable electrochemical sensor based on β-CD functionalized graphene for pH and potassium ion analysis in sweat. *Talanta* 2022;**245**:123481.

18. Maheswary T, Nurul AA, Fauzi MB. The insights of microbes' roles in wound healing: a comprehensive review. *Pharmaceutics* 2021;**13**:981.

19. Schuetz YB, Naik A, Guy RH, Kalia YN. Emerging strategies for the transdermal delivery of peptide and protein drugs. *Expet Opin Drug Deliv* 2005;**2**:533—48.

20. Iqbal B, Ali J, Baboota S. Recent advances and development in epidermal and dermal drug deposition enhancement technology. *Int J Dermatol* 2018;**57**:646—60.

21. Pereira R, Silva SG, Pinheiro M, Reis S, Vale ML. Current status of amino acid-based permeation enhancers in transdermal drug delivery. *Membranes* 2021;**11**:343.

22. Haque T, Talukder MMU. Chemical enhancer: a simplistic way to modulate barrier function of the stratum corneum. *Adv Pharmaceut Bull* 2018;**8**:169—79.

23. Ramadon D, McCrudden MTC, Courtenay AJ, Donnelly RF. Enhancement strategies for transdermal drug delivery systems: current trends and applications. *Drug Deliv Transl Res* 2022;**12**:758—91.

24. Bozuyuk U, Yasa O, Yasa IC, Ceylan H, Kizilel S, Sitti M. Light-triggered drug release from 3D-printed magnetic chitosan micro-swimmers. *ACS Nano* 2018;**12**:9617—25.

25. Chen CW, Liu YX, Wang H, Chen GP, Wu XW, Ren JA, et al. Multifunctional chitosan inverse opal particles for wound healing. *ACS Nano* 2018;**12**:10493—500.

26. Wong FSY, Tsang KK, Chu AMW, Chan BP, Yao KM, Lo ACY. Injectable cell-encapsulating composite alginate-collagen platform with inducible termination switch for safer ocular drug delivery. *Biomaterials* 2019;**201**:53—67.

27. Zuidema JM, Kumeria T, Kim D, Kang J, Wang J, Hollett G, et al. Oriented nanofibrous polymer scaffolds containing protein-loaded porous silicon generated by spray nebulization. *Adv Mater* 2018;**30**: 1706785.

28. Pritchard EM, Kaplan DL. Silk fibroin biomaterials for controlled release drug delivery. *Expet Opin Drug Deliv* 2011;**8**:797—811.

29. Rizi K, Green RJ, Donaldson MX, Williams AC. Using pH abnormalities in diseased skin to trigger and target topical therapy. *Pharm Res* 2011;**28**:2589—98.

30. Fu Y, Kao WJ. Drug release kinetics and transport mechanisms of non-degradable and degradable polymeric delivery systems. *Expet Opin Drug Deliv* 2010;**7**:429—44.

31. Abdullah HM, Farooq M, Adnan S, Masood Z, Saeed MA, Aslam N, et al. Development and evaluation of reservoir transdermal polymeric patches for controlled delivery of diclofenac sodium. *Polym Bull* 2022. Available from: https://doi.org/10.1007/s00289-022-04390-0.

32. Karpiński TM. Selected medicines used in iontophoresis. *Pharmaceutics* 2018;**10**:204.

33. Ita K. Perspectives on transdermal electroporation. *Pharmaceutics* 2016;**8**:9.

34. Banga AK, Bose S, Ghosh TK. Iontophoresis and electroporation: comparisons and contrasts. *Int J Pharm* 1999;**179**:1—19.

35. Chen X, Zhu L, Li R, Pang L, Zhu S, Ma J, et al. Electroporation-enhanced transdermal drug delivery: effects of log$P$, pKa, solubility and penetration time. *Eur J Pharmaceut Sci* 2020;**151**:105410.

36. Schoellhammer CM, Srinivasan S, Barman R, Mo SH, Polat BE, Langer R, et al. Applicability and safety of dual-frequency ultrasonic treatment for the transdermal delivery of drugs. *J Control Release* 2015;**202**:93—100.

37. Zhang S, Xin P, Ou Q, Hollett G, Gu Z, Wu J. Poly (ester amide)-based hybrid hydrogels for efficient transdermal insulin delivery. *J Mater Chem B* 2018;**6**:6723—30.

38. Chang M, Li X, Sun Y, Cheng F, Wang Q, Xie X, et al. Effect of cationic cyclopeptides on transdermal and transmembrane delivery of insulin. *Mol Pharm* 2013;**10**:951—7.

39. Feldstein MM, Tohmakhchi VN, Malkhazov LB, Vasiliev AE, Platé NA. Hydrophilic polymeric matrices for enhanced transdermal drug delivery. *Int J Pharm* 1996;**131**:229—42.

40. Tan HS, Pfister WR. Pressure-sensitive adhesives for transdermal drug delivery systems. *Pharmaceut Sci Technol Today* 1999;**2**:60—9.

41. Jung H, Kim MK, Lee JY, Choi SW, Kim J. Adhesive hydrogel patch with enhanced strength and adhesiveness to skin for transdermal drug delivery. *Adv Funct Mater* 2020;**30**:2004407.

42. Liu G, Zhou Y, Xu Z, Bao Z, Zheng L, Wu J. Janus hydrogel with dual antibacterial and angiogenesis functions for enhanced diabetic wound healing. *Chin Chem Lett* 2023;**34**:107705.

43. Cao D, Chen X, Cao F, Guo W, Tang J, Cai C, et al. An intelligent transdermal formulation of ala-loaded copolymer thermogel with spontaneous asymmetry by using temperature-induced sol—gel transition and gel—sol (suspension) transition on different sides. *Adv Funct Mater* 2021;**31**:2100349.

44. Martí-Centelles R, Dolz-Pérez I, De la OJ, Ontoria-Oviedo I, Sepúlveda P, Nebot VJ, et al. Two-component peptidic molecular gels for topical drug delivery of naproxen. *ACS Appl Bio Mater* 2021;**4**: 935—44.

45. Jiang H, Ochoa M, Waimin JF, Rahimi R, Ziaie B. A pH-regulated drug delivery dermal patch for targeting infected regions in chronic wounds. *Lab Chip* 2019;**19**:2265−74.

46. Dhal S, Verma P, Mishra M, Giri S. Oleogel-mediated transdermal delivery of white emitting NaYF4 conjugated with Rose Bengal for the generation of reactive oxygen species through NIR-upconversion. *Colloids Surf, B* 2020;**190**:110945.

47. Bao Z, Gu Z, Xu J, Zhao M, Liu G, Wu J. Acid-responsive composite hydrogel platform with space-controllable stiffness and calcium supply for enhanced bone regeneration. *Chem Eng J* 2020;**396**:125353.

48. Xu Y, Chen H, Fang Y, Wu J. Hydrogel combined with phototherapy in wound healing. *Adv Healthc Mater* 2022;**11**:2200494.

49. Li M, Liu X, Tan L, Cui Z, Yang X, Li Z, et al. Noninvasive rapid bacteria-killing and acceleration of wound healing through photo-thermal/photodynamic/copper ion synergistic action of a hybrid hydrogel. *Biomater Sci* 2018;**6**:2110−21.

50. Liu T, Chen M, Fu J, Sun Y, Lu C, Quan G, et al. Recent advances in microneedles-mediated transdermal delivery of protein and peptide drugs. *Acta Pharm Sin B* 2021;**11**:2326−43.

51. Yang J, Chen Z, Ye R, Li J, Lin Y, Gao J, et al. Touch-actuated microneedle array patch for closed-loop transdermal drug delivery. *Drug Deliv* 2018;**25**:1728−39.

52. Choi IJ, Kang A, Ahn MH, Jun H, Baek SK, Park JH, et al. Insertion-responsive microneedles for rapid intradermal delivery of canine influenza vaccine. *J Control Release* 2018;**286**:460−6.

53. Wang M, Han Y, Yu X, Liang L, Chang H, Yeo DC, et al. Upconversion nanoparticle powered microneedle patches for transdermal delivery of siRNA. *Adv Healthc Mater* 2020;**9**:1900635.

54. Bolton CJW, Howells O, Blayney GJ, Eng PF, Birchall JC, Gualeni B, et al. Hollow silicon microneedle fabrication using advanced plasma etch technologies for applications in transdermal drug delivery. *Lab Chip* 2020;**20**:2788−95.

55. Resnik D, Možek M, Pečar B, Janež A, Urbančič V, Iliescu C, et al. *In vivo* experimental study of noninvasive insulin microinjection through hollow si microneedle array. *Micromachines* 2018;**9**:40.

56. Yeung C, Chen S, King B, Lin H, King K, Akhtar F, et al. A 3D-printed microfluidic-enabled hollow microneedle architecture for transdermal drug delivery. *Biomicrofluidics* 2019;**13**:064125.

57. Jayaneththi VR, Aw K, Sharma M, Wen J, Svirskis D, McDaid AJ. Controlled transdermal drug delivery using a wireless magnetic microneedle patch: preclinical device development. *Sensor Actuator B Chem* 2019;**297**:126708.

58. Dong CW, Jeon JY, Kang HM, Park WT. Tip fabrication methods of hollow metal microneedles. *J Mech Sci Technol* 2023;**37**:261−9.

59. Chen Z, He J, Qi J, Zhu Q, Wu W, Lu Y. Long-acting microneedles: a progress report of the state-of-the-art techniques. *Drug Discov Today* 2020;**25**:1462−8.

60. Kim S, Yang H, Eum J, Ma Y, Fakhraei Lahiji S, Jung H. Implantable powder-carrying microneedles for transdermal delivery of high-dose insulin with enhanced activity. *Biomaterials* 2020;**232**:119733.

61. Li W, Terry RN, Tang J, Feng MR, Schwendeman SP, Prausnitz MR. Rapidly separable microneedle patch for the sustained release of a contraceptive. *Nat Biomed Eng* 2019;**3**:220−9.

62. Yang C, Sheng T, Hou W, Zhang J, Cheng L, Wang H, et al. Glucose-responsive microneedle patch for closed-loop dual-hormone delivery in mice and pigs. *Sci Adv* 2022;**48**:eadd3197.

63. Zhang Y, Wang J, Yu J, Wen D, Kahkoska AR, Lu Y, et al. Bio-responsive microneedles with a sheath structure for H_2O_2 and pH cascade-triggered insulin delivery. *Small* 2018;**14**:1704181.

64. Xu G, Lu Y, Cheng C, Li X, Xu J, Liu Z, et al. Battery-free and wireless smart wound dressing for wound infection monitoring and electrically controlled on-demand drug delivery. *Adv Funct Mater* 2021;**31**:2100852.

65. Lim C, Hong YJ, Jung J, Shin Y, Sunwoo S-H, Baik S, et al. Tissue-like skin-device interface for wearable bioelectronics by using ultra-soft, mass-permeable, and low-impedance hydrogels. *Sci Adv* 2021;**7**:eabd3716.

66. Li JS, Yang TR, Huang D, Chen YF, Huang YY, Li ZH. High-density microneedle array (hidma): an *in vivo* electroporation method for low-voltage gene delivery. *IEEE 33rd International Conference on Micro Electro Mechanical Systems (MEMS)* 2020:372−5. 2020.

67. Kusama S, Sato K, Matsui Y, Kimura N, Abe H, Yoshida S, et al. Transdermal electroosmotic flow generated by a porous microneedle array patch. *Nat Commun* 2021;**12**:658.

68. Xu C, Song Y, Han M, Zhang H. Portable and wearable self-powered systems based on emerging energy harvesting technology. *Microsyst Nanoeng* 2021;**7**:25.

69. Liu Z, Nie J, Miao B, Li J, Cui Y, Wang S, et al. Self-powered intracellular drug delivery by a biomechanical energy-driven tribo-electric nanogenerator. *Adv Mater* 2019;**31**:1807795.

70. Yang Y, Xu L, Jiang D, Chen BZ, Luo R, Liu Z, et al. Self-powered controllable transdermal drug delivery system. *Adv Funct Mater* 2021;**31**:2104092.

71. Cai X, Jiang Y, Lin M, Zhang J, Guo H, Yang F, et al. Ultrasound-responsive materials for drug/gene delivery. *Front Pharmacol* 2020;**10**:1650.

72. Soto F, Jeerapan I, Silva-López C, Lopez-Ramirez MA, Chai I, Xiaolong L, et al. Noninvasive transdermal delivery system of lidocaine using an acoustic droplet-vaporization based wearable patch. *Small* 2018;**14**:1803266.

73. Choi G, Fitriasari EI, Park C. Electro-mechanochemical gating of a metal−phenolic nanocage for controlled guest-release self-powered patches and injectable gels. *ACS Nano* 2021;**15**:14580−6.

74. Chen B, Wei J, Iliescu C. Sonophoretic enhanced microneedles array (SEMA)−improving the efficiency of transdermal drug delivery. *Sensor Actuator B Chem* 2010;**145**:54−60.

75. Ning X, Chen S, Yang Y, Hwang J, Wiraja C, Zhang C, et al. Photodynamic bubble-generating microneedles for enhanced transdermal cancer therapy. *ACS Appl Polym Mater* 2021;**3**:6502−12.

76. U.S. Food and Drug Administration. Transdermal and topical delivery systems−product development and quality considerations. 2019. Available from: https://www.fda.gov/regulatory-information/search-fda-guidance-documents/transdermal-and-topical-delivery-systems-product-development-and-quality-considerations.

77. Hu Y, Yang M, Huang H, Shen Y, Liu H, Chen X. Controlled ultrasound erosion for transdermal delivery and hepatitis B immunization. *Ultrasound Med Biol* 2019;**45**:1208−20.

78. Hu Y, Mo Y, Wei J, Yang M, Zhang X, Chen X. Programmable and monitorable intradermal vaccine delivery using ultrasound perforation array. *Int J Pharm* 2022;**617**:121595.

79. Wang H, Wang W, Li C, Xu A, Qiu B, Li F, et al. Flav7+DOX co-loaded separable microneedle for light-triggered chemo-thermal therapy of superficial tumors. *Chem Eng J* 2022;**428**:131913.

80. Watkinson AC. A commentary on transdermal drug delivery systems in clinical trials. *J Pharm Sci* 2013;**102**:3082−8.